Atmospheric Research 290 (2023) 106786

Contents lists available at ScienceDirect

Atmospheric Research

journal homepage: www.elsevier.com/locate/atmosres

The influence of the El Niño-Southern Oscillation phase transitions over the northern South America hydroclimate

Alejandro Builes-Jaramillo *, Juliana Valencia, Hernán D. Salas

Institución Universitaria Colegio Mayor de Antioquia, Facultad de Arquitectura e Ingeniería, Carrera 78 65 - 46 Bloque Patrimonial - Piso 2, Medellín, Colombia

ARTICLE INFO

Keywords:
ENSO
Tropical climate
Low-level jets
Caribbean
ChocoJet
Orinoco
Walker cells

ABSTRACT

The transitions between the phases of the El Nino-Southern Oscillation (ENSO) are abrupt changes in the Sea Surface Temperature (SST) conditions, which lead to opposite SST anomalies from the boreal winter of one year to the next boreal winter. In this work, we studied the influence of these transitions of ENSO over the general circulation and three Low-Level Jets (LLJs) over northern South America. We carry out a composite analysis of seasonal anomalies for climatic variables such as SSTs, vertical wind speed, precipitation, water vapor transport, and low-level winds to evaluate changes in the hydroclimatic features. We found that the ENSO phase transitions may induce changes in the vertical wind speeds associated with the Walker cells over the far-eastern Pacific Ocean, which gradually increases (reduces) their downward velocities during the transition from El Niño to La Niña (La Niña to El Niño), and increases(reduces) their upward velocity over northern South America. During the El Niño to La Niña transition (La Niña to El Niño), we found that the low-level water vapor transport changes over the zones of the Caribbean LLJ, the Orinoco LLJ, and the Chocojet with distinctive patterns during the transition years. Moreover, we found a precipitation dipole around the latitude 5°N over the far-eastern Pacific ocean (western Colombian coast) that persists throughout JJA and SON, especially for the El Niño to La Niña transition whereas negative precipitation anomalies predominate over the continental territory of northern South America during the La Niña to El Niño transition. This work contributes to the characterization of ENSO during its abrupt transitions and provides new information about the effects of those transitions on tropical hydro-climatology, which can be used to improve diagnosis, analysis, and modeling of the influence of ENSO over the far-eastern Pacific and northern South America.

1. Introduction

The El Niño-Southern Oscillation (ENSO) is a process consisting of an oceanic component (El Niño) and an atmospheric one (the Southern Oscillation) that occurs at inter-annual timescales. ENSO's oceanic component is associated with anomalous sea surface temperatures (SST) in the tropical Pacific Ocean, while its atmospheric component refers to changes in the sea level pressures along the tropical Pacific basin (Enfield and Mayer, 1997; Sarachik and Cane, 2010). The ENSO system has traditionally been classified into two main phases, one warm and the other cold, known respectively as El Niño (EN) and La Niña (LN), which are associated with anomalous increases (decreases) in SSTs in the central tropical Pacific and alterations in Walker's circulation (WC) (Philander, 1983; Rayner et al., 2003; Giannini et al., 2001). In addition, a more detailed analysis of the ENSO phases defines several ways to classify the events according to the region of the Pacific that changes its SST, which could be a Central Pacific or an Eastern Pacific event (Ashok and Yamagata, 2009).

In particular, over northern South America (NSA), ENSO modifies various meteorological processes related to convection induced by far eastern Pacific coastal warming and atmospheric perturbations resulting from Rossby waves and Walker circulation anomalies (Cai et al., 2020). Furthermore, several studies have shown evidence of a decrease (increase) in precipitation during El Niño (La Niña) over northeastern South America, while northwestern South America experiences the opposite alterations in precipitation, i.e., an increase (decrease) during El Niño (La Niña) (Grimm and Tedeschi, 2009; Poveda et al., 2011; Glantz and Ramirez, 2020). ENSO also affects the surface wind speeds and frequency of occurrence of the NSA Low-level jets (LLJs), the Caribbean LLJ (Wang, 2007), Orinoco LLJ (Builes-Jaramillo et al., 2022), and ChocoJet (Serna et al., 2018). These LLJs are associated with an increase (reduction) in water vapor transport, as well as divergent

* Corresponding author.
E-mail address: luis.builes@colmayor.edu.co (A. Builes-Jaramillo).

https://doi.org/10.1016/j.atmosres.2023.106786
Received 1 March 2023; Received in revised form 20 April 2023; Accepted 26 April 2023
Available online 3 May 2023

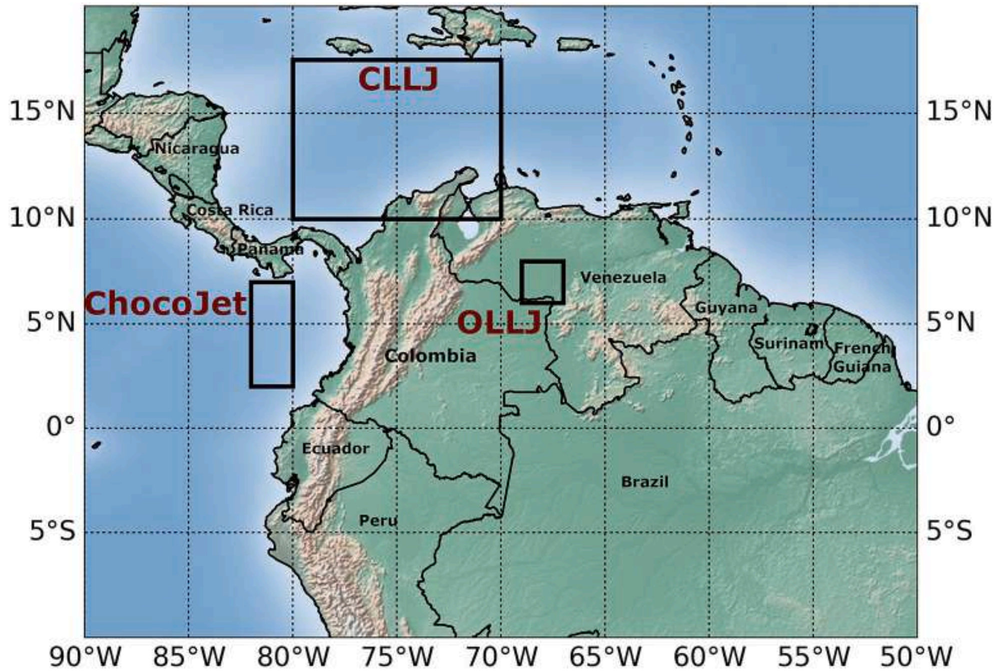

Fig. 1. Geographical location of the region of study over northern South America including the representative areas associated with the ChocoJet, CLLJ, and OLLJ.

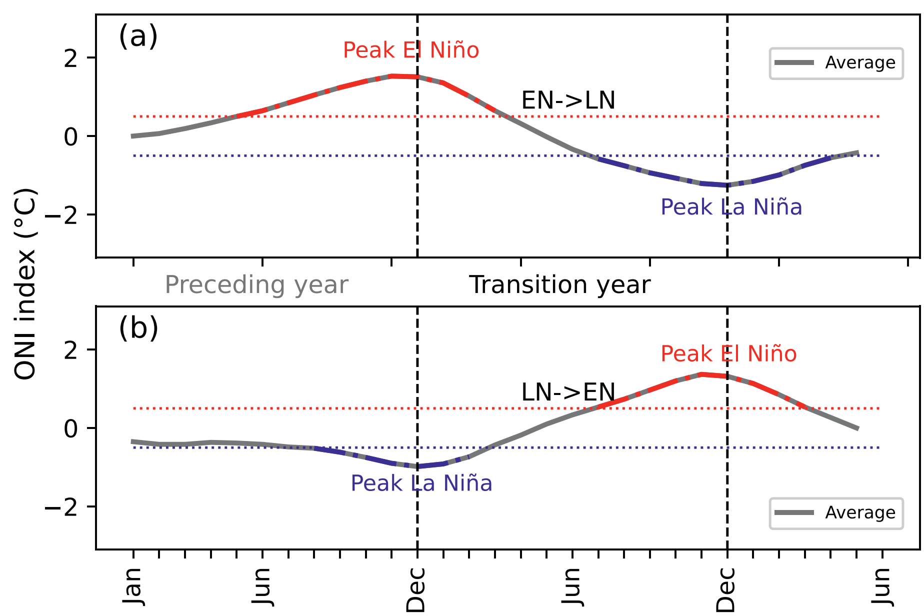

Fig. 2. ENSO phase transition according to the ONI index classification. (a) the EN→LN transition, and (b) LN→EN transition. (gray) average of EN→LN event transitions or LN→EN transitions. (light dotted blue) Threshold of the ONI index for the canonical LN (temperature anomalies below − 0.5 °C), and (light dashed red) Threshold of the ONI index for the canonical EN events. (dark dash blue) mean of the LN events. (dark dash red) mean of the LN events.

(convergent) winds linked to precipitation. The nature of these alterations in LLJs depends on their season of activity and the phase of ENSO. Moreover, ENSO is related to droughts or floods that cause severe ecological, socio-economic, and environmental impacts worldwide, depending on the phase and location of the region under study (Diaz et al., 2001; Cai et al., 2020).

The implications of ENSO transitions (from EN to LN or vice versa) on tropical hydroclimate are understudied. However, during the last decade, there has been a notable interest in their study, leading to diverse approaches for defining transitions. Wu et al. (2009) investigated the differences between atmospheric and oceanic features during boreal summers for ENSO-developing and ENSO-decaying conditions over the western North Pacific. Their results offer new findings on the relationships between ENSO-developing (ENSO-decaying) and the Walker circulation related to the cross-equatorial flow characteristics (anomalous anticyclone suppressing local rainfall). Warner and Moum (2019) defined four types of ENSO transitions in the western and equatorial tropical Pacific cold tongue (denoted as EN–warming, EN–cooling, LN–warming, LN–cooling), based on the magnitude of the ONI index and the temporal gradient of ONI. Their approach helps to identify that the mixing of oceanic waters (or lack of it) contributes to the heating of the sea surface during transitions to peak EN and cooling during transitions to peak LN. Hence, according to the authors, this oceanic mixing acts as a positive feedback mechanism for developing EN

Table 1
Years of EN→LN and LN→EN ENSO transitions during the 1959–2022 period.

Transition	Transition year	El Niño event	La Niña event
EN→LN	1964	1963	1964
	1960	1969	1970
	1973	1972	1973
	1983	1982	1983
	1988	1987	1988
	1995	1994	1995
	1998	1997	1998
	2005	2004	2005
	2007	2006	2007
	2010	2009	2010
Transition	**Transition year**	**La Niña event**	**El Niño event**
LN→EN	2016	2015	2016
	1965	1964	1965
	1972	1971	1972
	1976	1975	1976
	2006	2005	2006
	2009	2008	2009
	2018	2017	2018

and LN events.

Bahrami et al. (2020) studied the impact of two types of ENSO transitions (El Niño to La Niña and La Niña to El Niño) on atmospheric circulation, rainfall, and temperatures in the Middle East during boreal autumn. They found that during EN to LN (LN to EN) transitions, the Sea Level Pressure structure over the Atlantic region changes, with a minimum (maximum) between the Iceland low and the Azores high. These conditions are associated with enhanced (decreased) rainfall over most parts of the Middle East. Fang (2020) defines ENSO transitions based on changes from the prior year to the current year as cyclic, episodic, and multi-year, which correspond to LN to EN, Neutral to EN, and EN to EN (with a similar classification for LN). This work argues that, for example, multi-year La Niña events can shift the region of reduced precipitation to the southeast in the US more than other La Niña events. The author also argues that during the summer, cyclic La Niña events can generate distinct atmospheric wave trains to the extratropical Pacific and cause a significant warming signal over the Midwest in the US compared to multi-year La Niña events.

Mokhov and Timazhev (2022) have defined nine types of ENSO transitions, including Neutral to EN, Neutral to LN, and Neutral to Neutral, which they classify as a continuation of Neutral conditions. They argue that their approach is useful in obtaining predictive estimates of the risk of anomalous regional weather and climatic conditions using predictive model simulations for the evolution of the ENSO processes. Specifically, their approach can be used to estimate anomalously high Surface Air Temperature values in May-June-July in Asian Russia regions for the EN to EN transition. Additionally, they estimate that positive temperature anomalies have been increasing (from 80 up to 100%), including extremely high values, in the spring-summer months in European Russia regions for the EN to LN transition and Asian Russia regions for the EN to EN transition. These findings demonstrate that studying ENSO transitions can provide new insights into the effects of ENSO on atmospheric processes worldwide. However, all previous works have been based on limited data records and use non-unified definitions of ENSO transitions.

Acknowledging the limitations imposed by the few recorded ENSO transition episodes in historical datasets and the absence of prior studies on the influence of such transitions in the region, this study addresses the following questions: (1) What are the changes in vertical wind speed associated with the Walker cells during ENSO transitions?; (2) Do the ENSO phase transition years alter precipitation and water transport in NSA in contrast to ENSO-neutral conditions?; and, (3) Do the surface wind speed patterns associated with the Low-level jets, during their most active seasons, change during ENSO transitions in relation to neutral ENSO conditions?. To tackle these questions, we analyze the anomalies of sea surface temperatures (SST), vertical wind speeds, precipitation, and water vapor transport (WVT), and the wind speed anomalies of three Low-level Jets in their seasons of activity over NSA during the ENSO transition years.

This work is organized as follows: Section 2 describes the study region and datasets. Section 3 presents the methods in detail, including the composite analysis, the definition of ENSO transitions, and the comparative analysis procedure. Section 4 presents the results and discussion. Finally, 5 provides conclusions and outlines future work.

2. Study region and data

The study region is defined by the coordinates 50°W–90°W and 10°S-

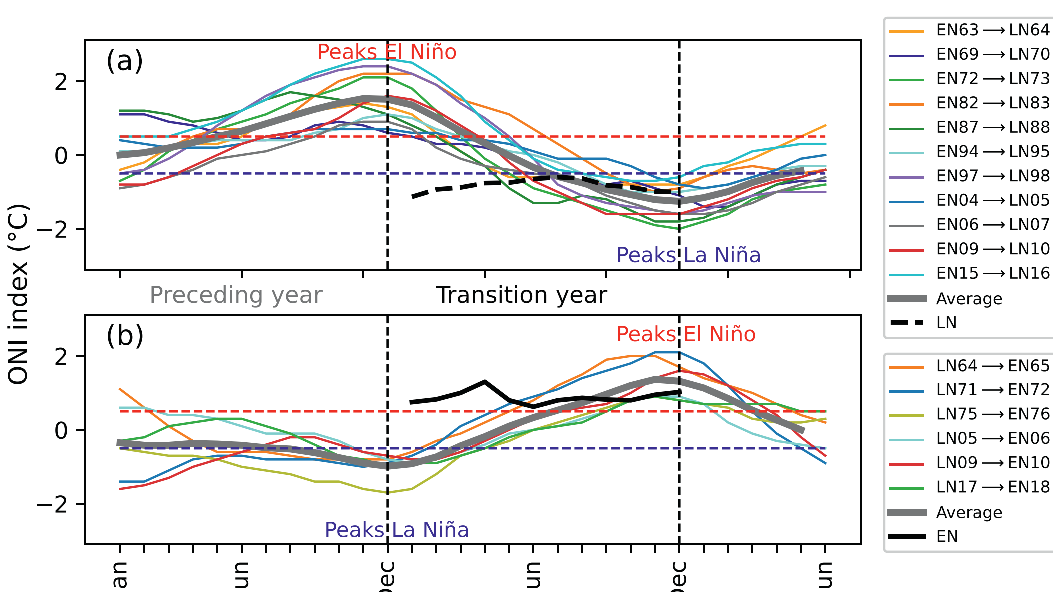

Fig. 3. ENSO phase transitions according to the ONI index classification. (a) the EN→LN transition, and (b) LN→EN transition. Threshold of the ONI index for the canonical LN (dashed blue) and EN (dashed red) events. The multi-annual mean of the canonical phase (a) LN and (b) EN, black dotted line, and black line, respectively. (gray) average of all the ONI events classified.

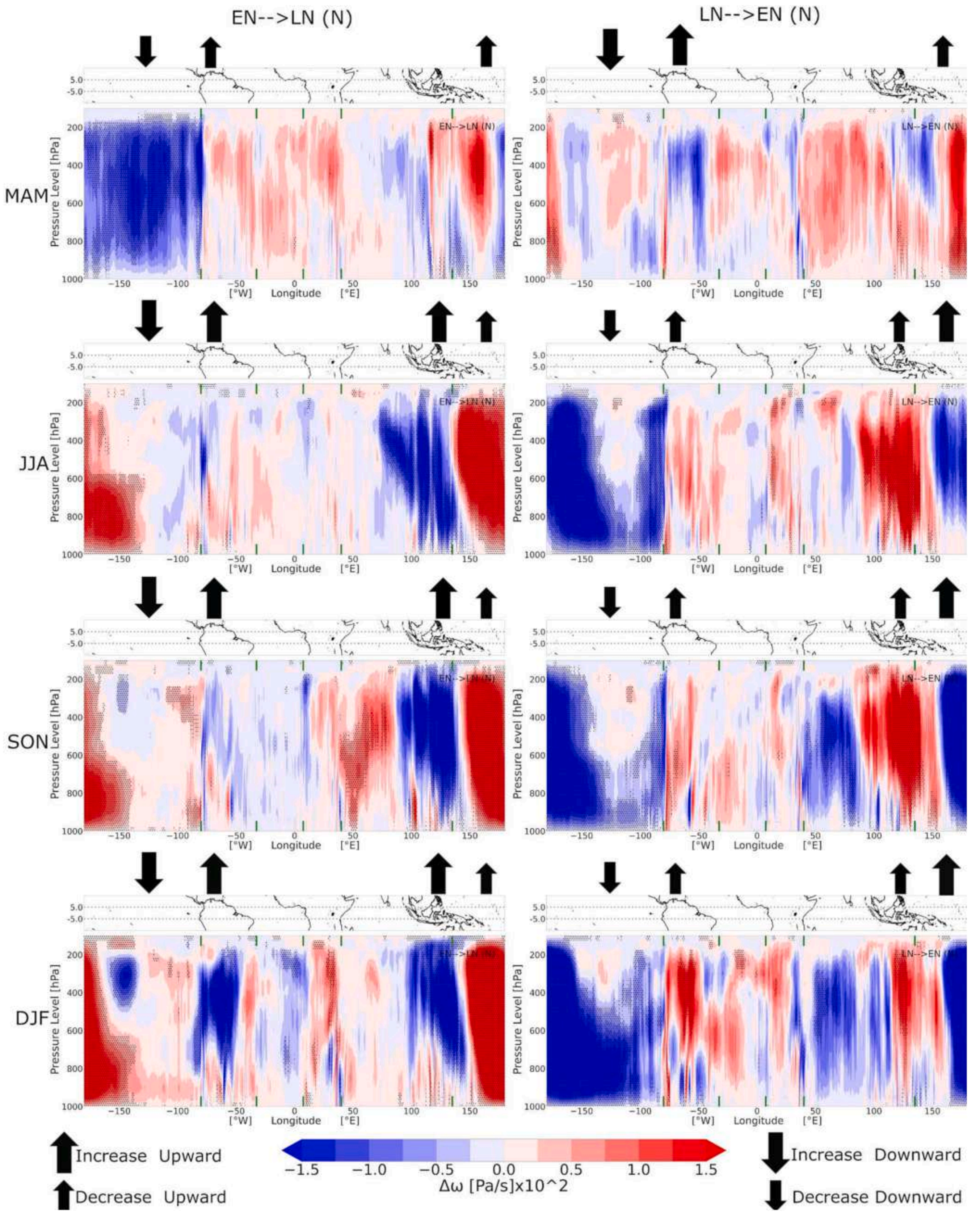

Fig. 4. Seasonal anomalies of the vertical velocity of winds (ω) during phase transition year minus the Neutral phase of ENSO (N) over the 5°N - 5°S. (left) EN→LN transition minus N and (right) LN→EN minus N.

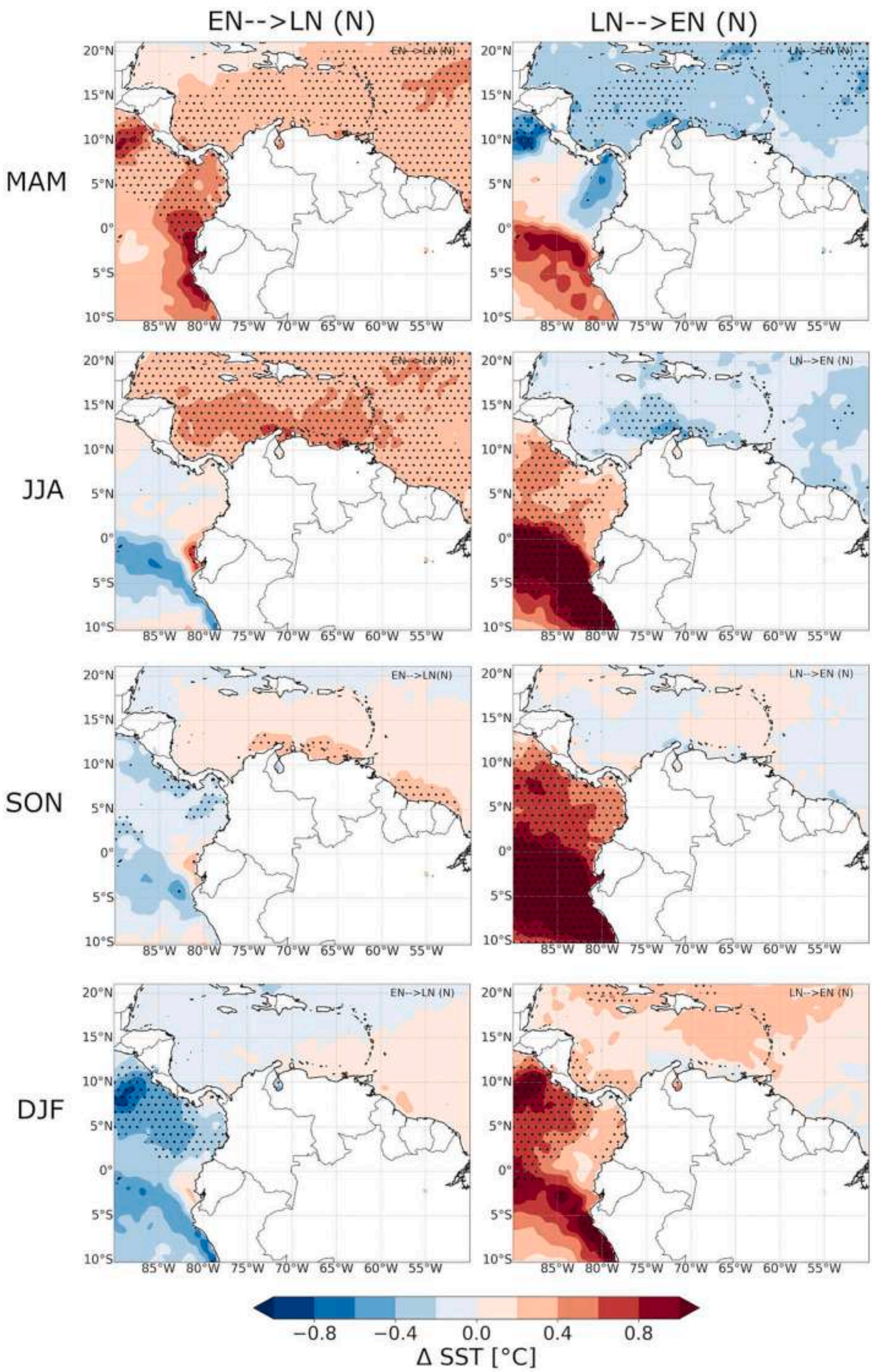

Fig. 5. Seasonal Sea Surface Temperatures anomalies for ENSO phase transition minus neutral ENSO conditions. Gray dots denote the zones with statistical significance according to the t-test at the significance level of 0.05.

20°N, covering the NSA region. The Low-Level jets (LLJ) studied in this research are located in areas (as shown in Fig. 1) associated with the higher activity of the Caribbean LLJ (CLLJ) (12.5°W–17.5°N, 80°W–70°W) (Wang, 2007); the Choco LLJ (ChocoJet) (2°N–7°N, 82°N–80°W) based on (Sierra et al., 2021; Cerón et al., 2020), and the Orinoco LLJ (OLLJ) (6°N–8°N and 67°W–69°W) (Builes-Jaramillo et al., 2022). We use data from SST, zonal and meridional wind speed, vertical wind speed (ω) from the pressure levels 1000 hPa to 700 hPa, precipitation, and specific humidity provided by the ERA5 atmospheric reanalysis (Hersbach et al., 2020), for the period 1959–2022, a monthly time scale and a 0.25° x 0.25° grid size.

3. Methods

3.1. ENSO transitions

First, to define the canonical phases of ENSO (EN and LN), we used the Oceanic Nino Index (ONI) classification by the United States Climate Prediction Center. This classification defines EN (LN) when the five running three-month seasons' average of the SST is above + 0.5 °C

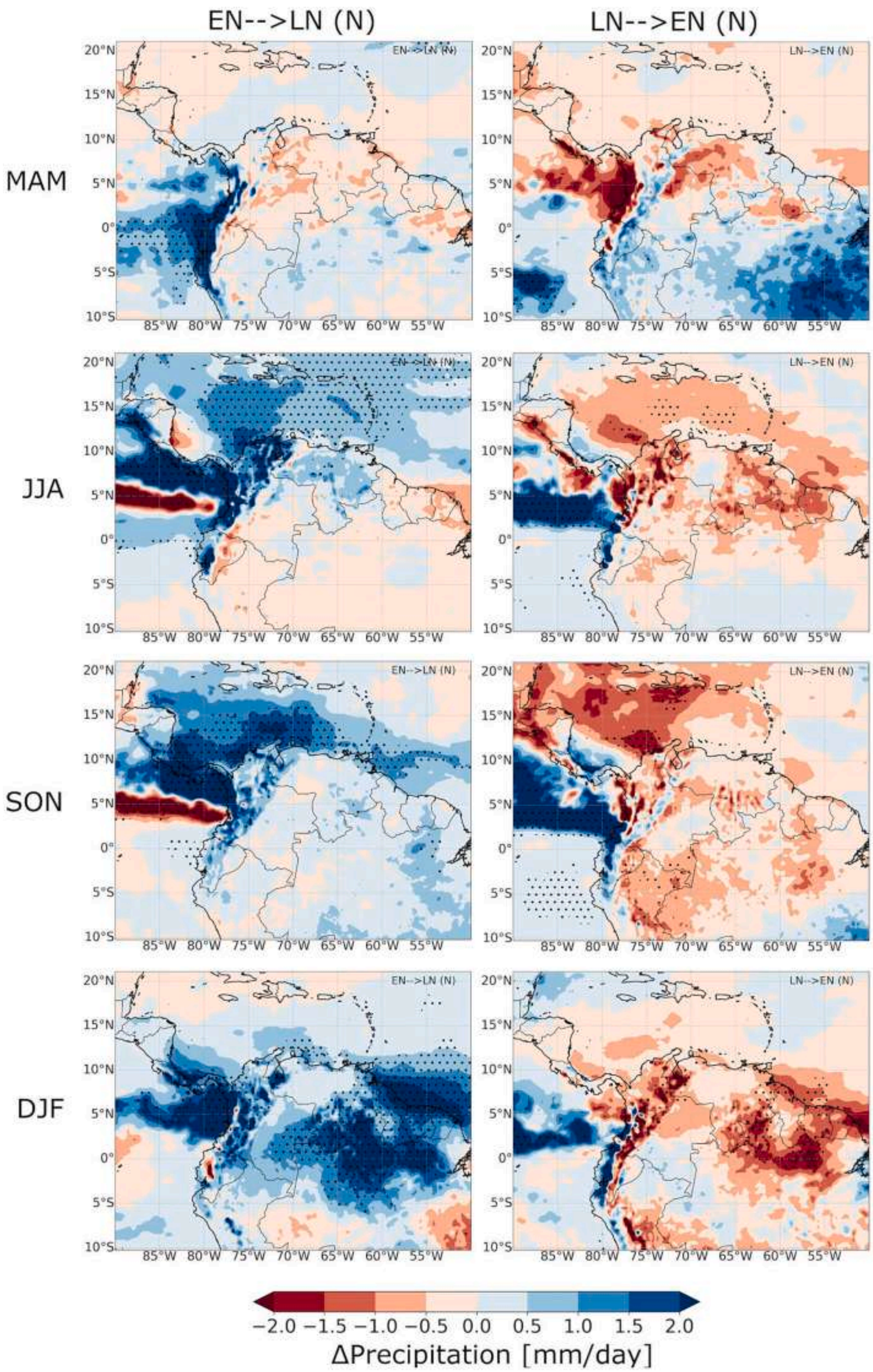

Fig. 6. Precipitation anomalies during ENSO phase transition minus neutral condition for the four trimesters of the year. Gray dots depict the coordinates with statistical significance according to the t-test.

(below − 0.5 °C) in the Niño 3.4 zone, then the canonical EN (LN) occurs (NOAA, 2022).

Second, we define transitions based on the works by Bahrami et al. (2020) and Mokhov and Timazhev (2022), which state that most EN events reach their peaks in the boreal late autumn or early winter, while all LN events tend to occur in the boreal late spring or summer, peaking in late boreal autumn or early winter. Considering these factors, we revise the ONI index by identifying changes from El Niño to La Niña [hereafter EN→ LN] as well as changes from La Niña to El Niño [hereafter LN→ EN]. Hence, years, where there is a change from EN → LN or vice versa from boreal winter (prior year) to boreal winter (next year) are classified as transition years. Fig. 2 illustrates the definition of a transition year as the year when the canonical ENSO turns from EN to LN or vice versa.

3.2. Composite analysis

We use the seasonal composite analysis method (Boschat et al., 2016; Xie et al., 2017) to study the anomalies of climatic variables including wind speed, precipitation, and water vapor transport during the ENSO

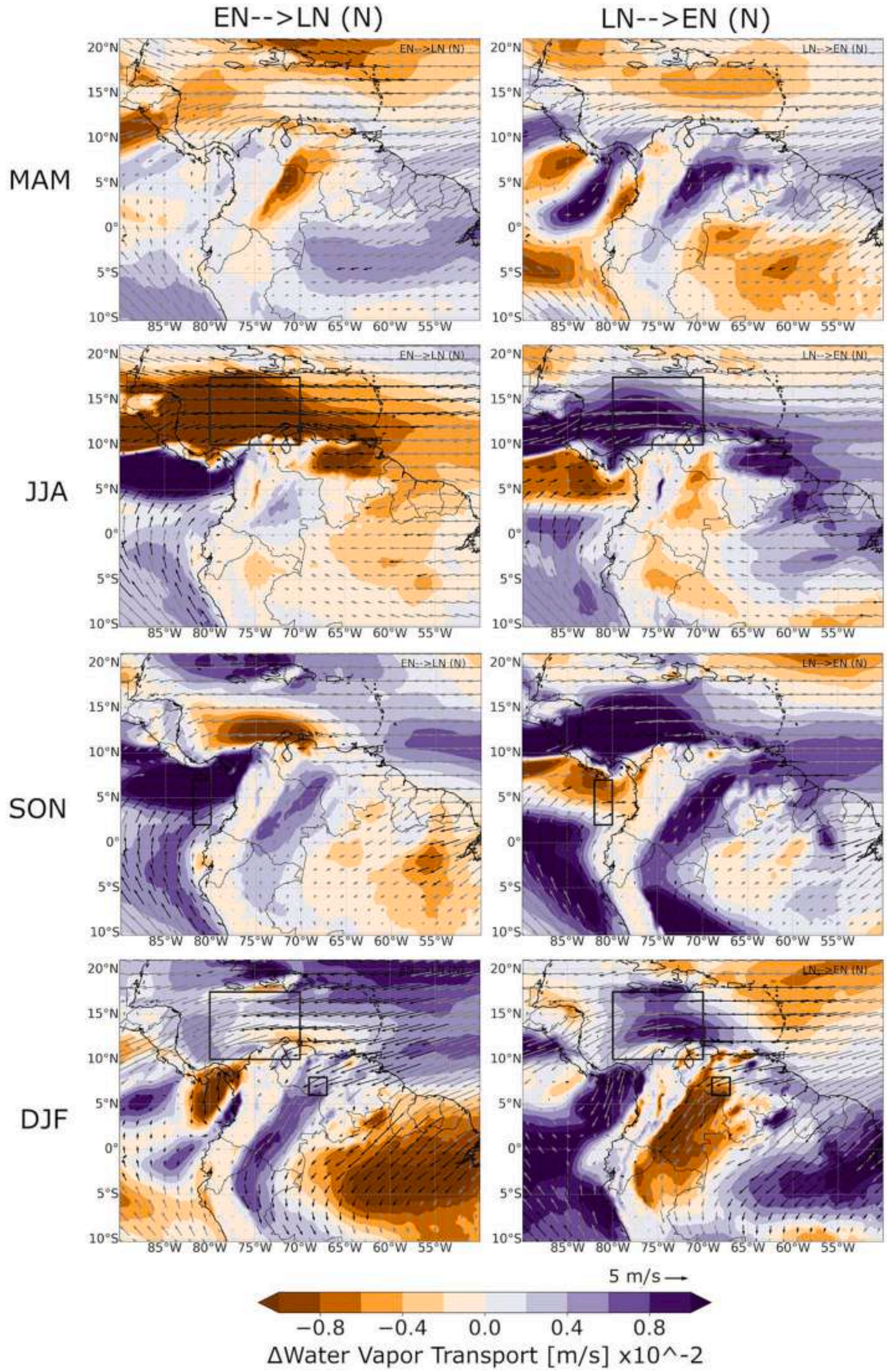

Fig. 7. Seasonal anomalies of water vapor transport (WVT) and wind speed for northern south America for ENSO transitions minus neutral conditions at 925 hPa. The boxes highlight the region associated with the LLJs during its season of high activity. Black arrows denote locations where winds speed at 925 hPa during transitions is statistically different from the canonical phases according to the t-test at the significance level of 0.05.

transition years compared to the ENSO Neutral condition (N). To compute the composite we follow the next steps: (1) we define the months for each ENSO phase transition year and the months in canonical Neutral events according to the ONI index; (2) we isolate the climatic variables for the months in transition years previously defined, as well as for the canonical ENSO event, which constitutes the keytimes; (3) we isolate the climatic variables and compute the average and anomalies for all key-times; and finally, (4) we use the t-student test to verify whether there is a significant anomaly between the ENSO transitions years and the neutral condition. In particular, we calculate two anomalies for each climate variable, EN→LN minus N [hereafter EN→LN (N)] and LN→EN minus N [hereafter LN→EN (N)].

Moreover, we analyze the surface wind speeds associated with each LLJ during its active season. Hence, we compute composites for Choc-oJet during September-October-November (SON), for the CLLJ during June-July-August (JJA) and December-January-February (DJF), and for the OLLJ during DJF.

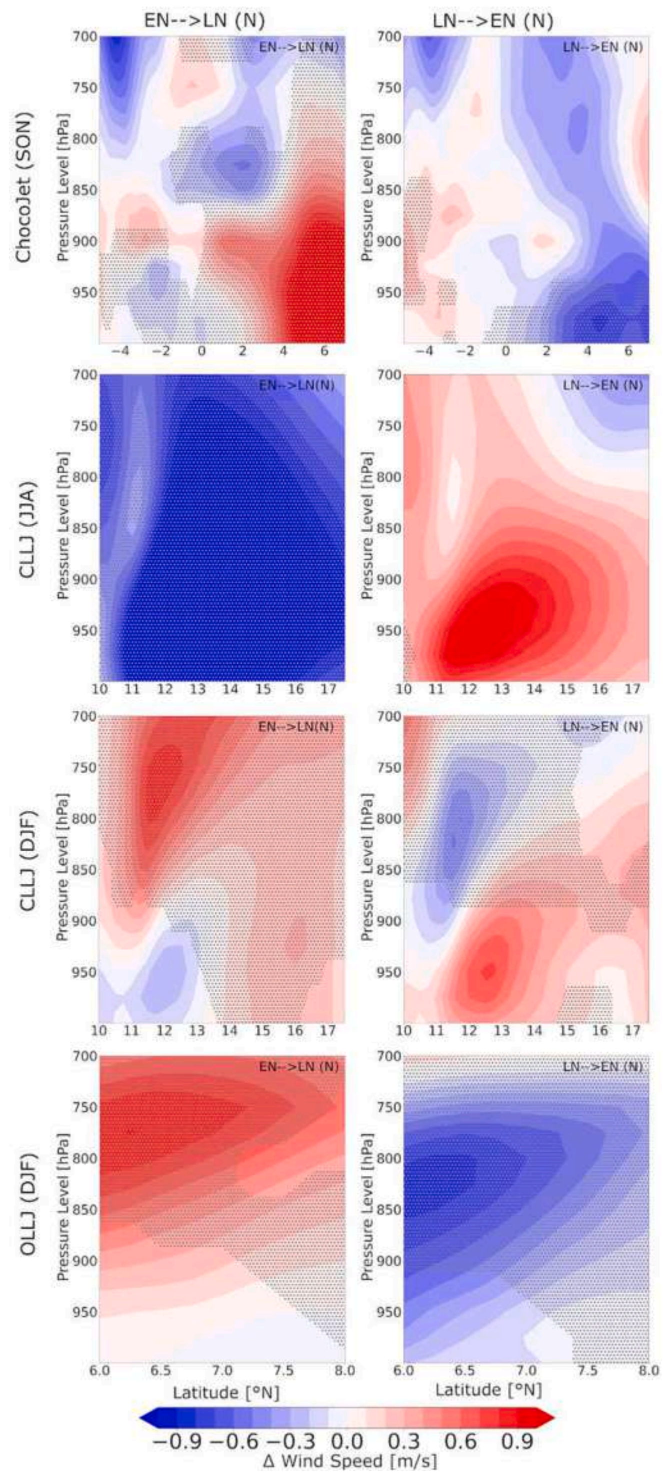

Fig. 8. Atmospheric cross-section of wind speed anomalies of ENSO transitions minus ENSO canonical phases from 1000 hPa to 700 hPa for the zones associated with the LLJs (Fig. 1) during its season of high activity. Gray dots depict the coordinates with statistical significance according to the t-test at the significance level of 0.05.

4. Results

4.1. ENSO transitions

Following the ENSO phase transition classification mentioned in Section 3.1, we identified eleven EN→LN transitions and six LN→EN transitions during the 1959–2022 period (Table 1). These transitions were selected based on the mature conditions of one phase of ENSO at the end of the first year (preceding year) and the mature opposite phase (transition year) at the end of the second year, as illustrated in Fig. 3. Fig. 3a also presents the composite for the EN→LN transition as well as the composite for the canonical LN events. Additionally, Fig. 3b shows the composite for the LN→EN transition and the composite for the canonical EN events. Fig. 3 evidences the abrupt decrease (increase) of SST anomalies for the EN→LN (LN→EN) transition in one year, during which the SST anomalies can change from $\sim +2^{o}C$ to $\sim -2^{o}C$ ($\sim -2^{o}C$ to $\sim + 2^{o}C$).

The Walker circulation is one of the main drivers of the atmospheric feedback of ENSO (Bayr et al., 2020), and it is primarily influenced by the SST differences between the eastern and the warm pool of the western Pacific Ocean (Philander, 1990). Fig. 4 shows the seasonal mean vertical velocity anomalies over the 5°N - 5°S region for the ENSO phase transition years minus the neutral conditions over the region (climatology of the 1959–2022 period). During MAM, for the EN→LN transition (Fig. 4 left), the downward wind velocities decrease in the atmospheric column (1000 hPa - 200 hPa) in the far-eastern Pacific (FEP) region (-100°W and −180°W) and the Indo Pacific. Furthermore, there are upward wind velocities over the NSA and the Tropical Atlantic basin, which contrast with the neutral conditions (Appendix A Fig. 11). During JJA, the downward wind velocity significantly increases from −180°W to −140°W between the atmospheric pressure levels 1000 hPa to 600 hPa. This pattern is repeated for SON and DJF, while for DJF, the downward wind velocity decreases from 400 hPa to 200 hPa at the longitude −150°W. For the seasons JJA, SON, and DJF, the upward wind velocities increase over the NSA continental territory.

During the MAM season, for the LN→EN transition (Fig. 4 right), the FEP region shows an increase in downward wind velocities between longitudes of −100°W and −150°W, while upward wind velocities increase over the NSA and Tropical Atlantic basin. In contrast, during JJA, SON, and DJF, the FEP zone shows a reduction in downward wind velocities covering the atmospheric column from around −120°W to −180°W. Additionally, upward wind velocities decrease over the NSA and Atlantic (Appendix A Fig. 12).

Previous studies have shown that changes in the Walker cell over the tropical Pacific are primarily observed in the central and FEP zones, where ENSO develops in response to changes in SST and atmospheric circulation patterns. These alterations in the upward (downward) circulation branches of the Walker cell could be associated with stronger (weaker) Pacific trade winds (Bayr et al., 2018), a reduction (increase) of equatorial Atlantic precipitation (Sasaki et al., 2015; Saravanan and Chang, 2000; Tedeschi and Sampaio, 2022), and feedback from surface net heat fluxes (Guilyardi et al., 2009).

The SST anomalies over the tropical Pacific Ocean are a distinguishing characteristic of ENSO (Gill, 1980; Bjerknes, 1969; Wang and Picaut, 2013), with its warm (EN) and cold (LN) canonical phases associated with higher (lower) SSTs than normal conditions. Although these patterns have been extensively studied for the ENSO canonical phases (EN - LN), the changes in SSTs for the transitions EN→LN and LN→EN in relation to the neutral ENSO conditions have been understudied. Fig. 5 shows the composite seasonal SST anomalies during the ENSO transitions relative to neutral conditions years. During the EN→LN, there are positive SST anomalies, which gradually change to negative SST anomalies in DJF over the Pacific coasts of Peru, Ecuador, and Colombia. In contrast, during LN→EN from MAM to DJF, positive SST anomalies exhibit an uninterrupted increase.

During the EN→LN (LN→EN) transition, the SSTs anomalies increase (decrease) in MAM and JJA over the Caribbean Sea, while there is a gradual decrease (increase) from SON to DJF. A remarkable feature during the LN→EN transition is that over the Pacific basin, positive SST anomalies persist throughout the year with a progressive increase. We used the Hadley Centre Global Sea Surface Temperature dataset (Rayner et al., 2003) to obtain these results, which were consistent with ERA5

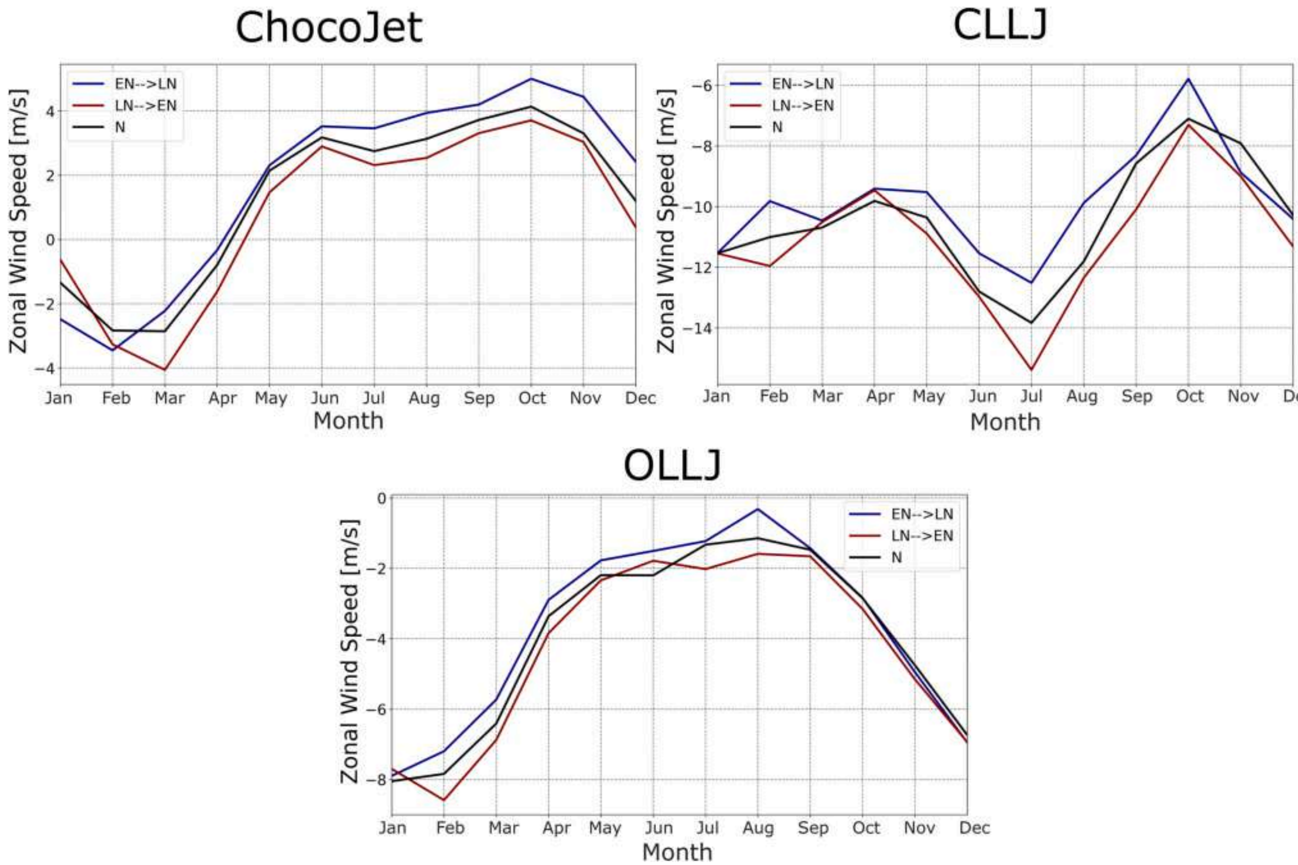

Fig. 9. Annual cycle of zonal wind speed over the Chocojet, CLLJ, and OLLJ regions for the 925 hPa level.

(not shown).

4.2. Precipitation and water vapor transport during the ENSO transitions

Fig. 6 shows the composites of seasonal precipitation anomalies for ENSO transition years. During the EN→LN transition in MAM, precipitation increases over the Pacific coast of northern Peru, Ecuador, and western Colombia. In contrast, precipitation reduces over the Orinoco River basin during this transition. During JJA and SON, precipitation exhibits a dipole over the FEP region, with a latitudinal band (north of) around 5°N showing a decrease (increase) in precipitation anomalies. During SON, this dipole is more evident, with higher precipitation anomalies over Central America. During DJF, positive precipitation anomalies cover the Colombian Pacific coast, the western Andean mountain range, and the northern Amazon River basin.

During the LN→EN transition in MAM, precipitation decreases over the Pacific coast and the FEP. In particular, negative precipitation anomalies appear on the western coast of Colombia, Ecuador's central Andes, and the Orinoco River plains between Colombia and Venezuela. Furthermore, precipitation decreases over the Caribbean Sea while increasing over the northeast Amazon River basin and the Andean region. During JJA, precipitation anomalies show a dipole between the western Pacific coast of Colombia and northern central America, where precipitation anomalies increase over FEP and Ecuador's Pacific coast (below the latitude 5°N). For the northernmost part of the continental territory and the Caribbean Sea, there is a reduction of precipitation, but the higher anomalies occur in the Andes and Guianese shield. Moreover, during SON, the positive anomalies of precipitation in the FEP region reach up to 10°N latitude and some portion of the Atlantic coasts in Central America, while there are higher negative anomalies over the Caribbean Sea, northern Peru, and northern Brazil. During DJF, the increased precipitation over the FEP weakens and maintains over a 5°N to 0°N latitudinal band. Additionally, there is a reduction in precipitation over the Andean mountain range from northern Colombia to central Peru and a negative precipitation anomaly intensification over the Guianese shield.

During the EN→LN transition, positive anomalies are observed over the NSA Andes and the Caribbean from the JJA season through DJF. This feature even covers the Orinoco basin and the northern Amazon and induces an abrupt change from the dry conditions related to EN. Such changes in mountainous regions like the Andes can be related to flood or landslide events (Shi et al., 2021; Wang et al., 2021). In addition, during the LN→EN transition, there is a pattern of negative precipitation anomalies from the Caribbean to all of NSA. Lower precipitation is consolidated over northeast Colombia and the Orinoco basin from SON to DJF, which might be related to a drier onset of the South American Monsoon System (de Carvalho and Cavalcanti, 2016), meaning less precipitation over the Amazon basin. Precipitation patterns over NSA are coherent with the vertical wind speed anomalies shown in Fig. 5. For the EN→LN (LN→EN) transition phase, there is an increased (reduced) upward wind speed that may be related to positive (negative) anomalies of precipitation over NSA. Perturbations of the Pacific Walker circulation are related to changes in the convection patterns over the Pacific Ocean and also over NSA and Africa (Bayr et al., 2020; Rao et al., 1998; Oliver, 2005).

Fig. 7 presents the seasonal anomalies of water vapor transport (WVT) and wind speed at 925 hPa for the ENSO phase transitions compared to neutral conditions. During the EN→LN transition in MAM, there is a reduction of WVT over the OLLJ corridor. There are also changes with respect to neutral conditions, but with lower significance and magnitude. These results for MAM could be related to the increase of SSTs (Fig. 5) and precipitation over the Pacific coast and Caribbean sea, which may induce a reduction of the moisture availability to be transported by the LLJs. During JJA, there is a reduction (increase) of WVT

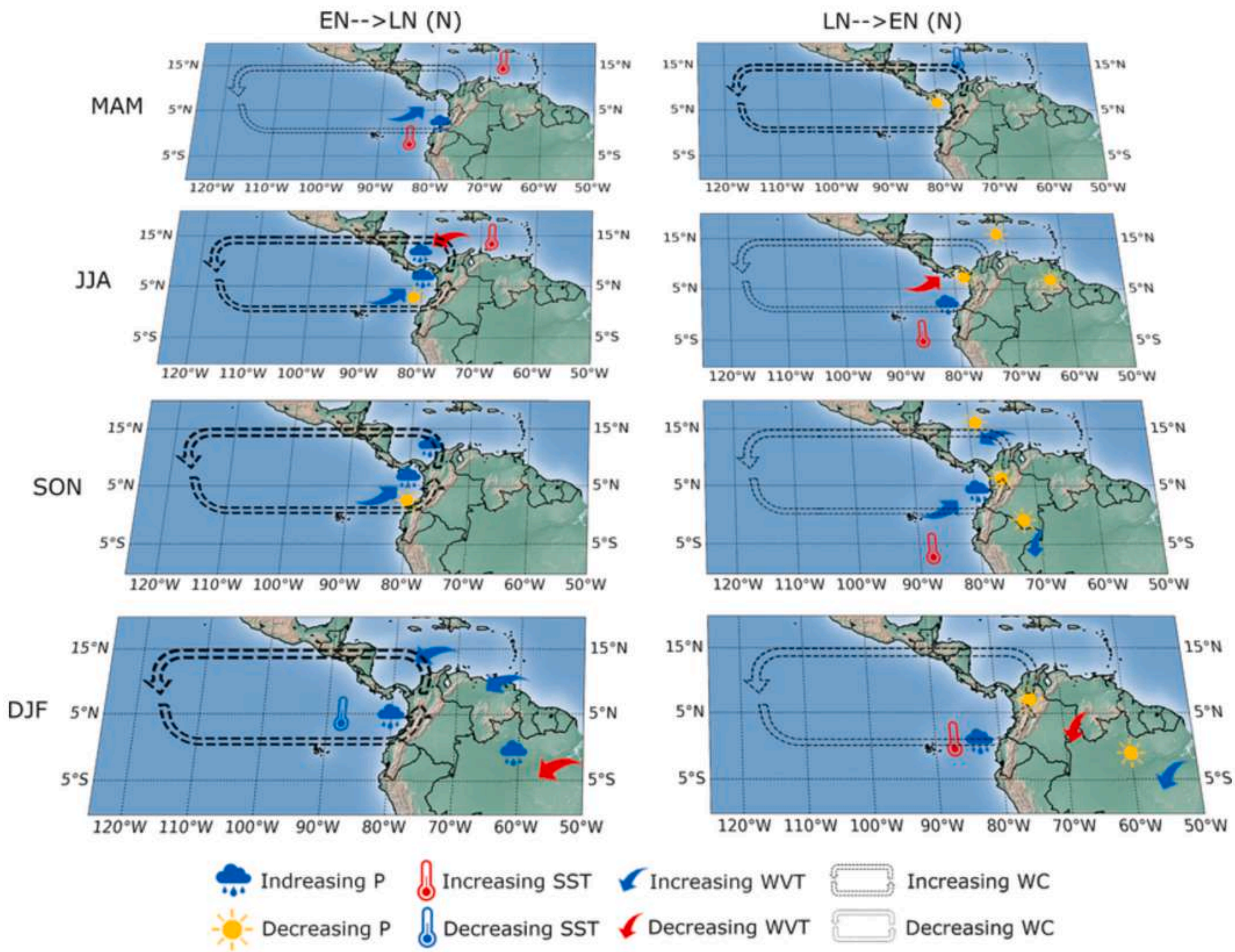

Fig. 10. Schematic depiction of changes in the Walker Circulation from −150°W to −50°W and the statistically significant changes during each season over northern South America for the EN→LN and LN→EN phase transitions.

over the Caribbean during the active season of the CLLJ, while in SON, the increase in WVT over FEP is concomitant with the active season of the Chocojet, and there is an increased WVT over the OLLJ corridor. During DJF, there are higher wind speed anomalies over the OLLJ entrance region, and the enhanced WVT over the OLLJ corridor is one important source of moisture toward the Amazon river basin. In contrast, the northeast of the Amazon river basin experiences a reduction in WVT during this season.

During the MAM season, the LN→ transition shows an increase in WVT over the OLLJ and the Panama LLJ, but a reduction over the Papagayo LLJ, as reported by Romero-Centeno et al. (2007) and Ordóñez-Zúñiga et al. (2021). In JJA, there is an increase in WVT over the Caribbean Sea, which continues into SON. During this season, the WVT anomalies increase over the OLLJ corridor, but decrease over the ChocoJet pathway into the continent. In DJF, WVT decreases over the OLLJ corridor, which is its most active season. At the same time, WVT anomalies increase over the northeast Amazon, while the CLLJ winds shift towards the Pacific over Panama. The LN→EN transition shows an increase in WVT anomalies over the Pacific coast during JJA and SON, coinciding with an increase in observed precipitation, as shown in Fig. 5.

This could be associated with the physical barrier imposed by the westernmost Andes Mountains, outside the ChocoJet's highest activity season (Yepes et al., 2019). During SON, the ChocoJet region shows a WVT increase (decrease) during EN→LN (LN→EN). In DJF, WVT reduces (increases) for the EN→LN (LN→EN) transition over the CLLJ region.

A notable feature of the EN→LN transition is the positive WVT anomalies along the OLLJ corridor during SON and the negative precipitation anomalies over northern South America. This regime could induce a penetration of the South America Low-Level Jet (SALLJ) over the Southeast South America (SESA) region with increased WVT, leading to more intense precipitation events in the Argentina and Bolivia Andes (Nesbitt et al., 2021; Sasaki et al., 2022).

4.3. Wind speed of the LLJs during the ENSO transitions

Fig. 8 shows the anomalies in wind speeds during ENSO transitions compared to neutral conditions in the seasons when the ChocoJet, CLLJ, and OLLJ are active. During SON, LN→EN transition causes a reduction in wind speed from 2°N to 7°N between 1000 hPa to 850 hPa in the Chocojet region, while the EN→LN transition increases wind speed in the same area. These results agree with those in Fig. 7, which show reduced (increased) south-easterlies on the northern Pacific coast of Colombia, between latitudes 4°N and 6°N for the LN→EN (EN→LN) transitions.

During the active seasons of the CLLJ (JJA and DJF), for both transitions, there is evidence of changes in the magnitude of wind speed. For JJA, the vertical structure of wind speed anomalies increases (decreases)

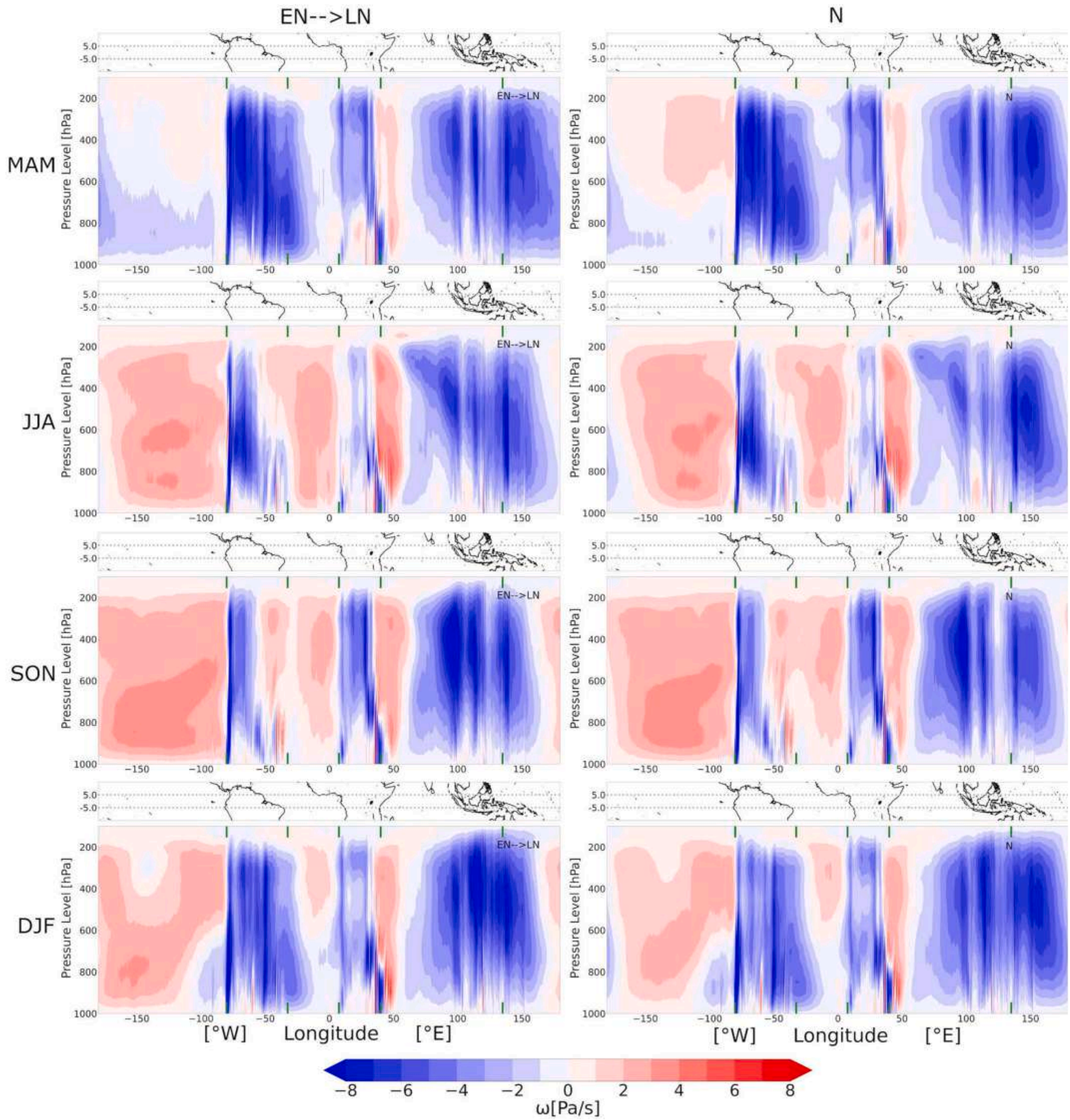

Fig. 11. Seasonal climatology of the vertical velocity of winds, ω, over the 5°N - 5°S region for (left) EN→LN phase transition and (right) N neutral phase.

from the 1000 hPa to 800 hPa pressure levels for the LN→EN (EN→LN) transition. In DJF, there is a dipole in the vertical distribution of wind speed anomalies at the CLLJ region, with an increase (reduction) in the lower atmospheric levels (1000 hPa to 900 hPa) and a reduction (increase) in wind speeds between 900 hPa and 750 hPa atmospheric levels around latitudes 10°N and 14°N for the LN→EN (EN→LN) transition.

In DJF, wind speeds decrease (increase) for the LN→ EN (EN→ LN) transitions in the OLLJ. In both cases, the higher anomalies occur at latitudes 6.0°N and 8.0°N between 900 hPa to 700 hPa atmospheric levels. This result may not be related to the jet's conditions in particular but to the boundary conditions provided by the easterlies, which are the predominant wind structure in the region above 850 hPa.

The profiles of vertical wind speeds in the areas defined for the ChocoJet, CLLJ, and OLLJ (See Fig. 1) confirm the features mentioned in the literature for the canonical ENSO phases, such as the decrease (increase) of winds at 950 hPa of the CLLJ during LN (EN) in JJA (Wang, 2007); the increase (decrease) of wind speed at 925 hPa of the ChocoJet during LN (EN) in SON (Sierra et al., 2021); and the slight decrease (increase) in wind speed at 950 hPa of the OLLJ during EN (LN) in DJF (Builes-Jaramillo et al., 2022). However, our analysis of vertical profiles during the EN→LN and LN→EN does not show any differences compared to neutral conditions (not shown).

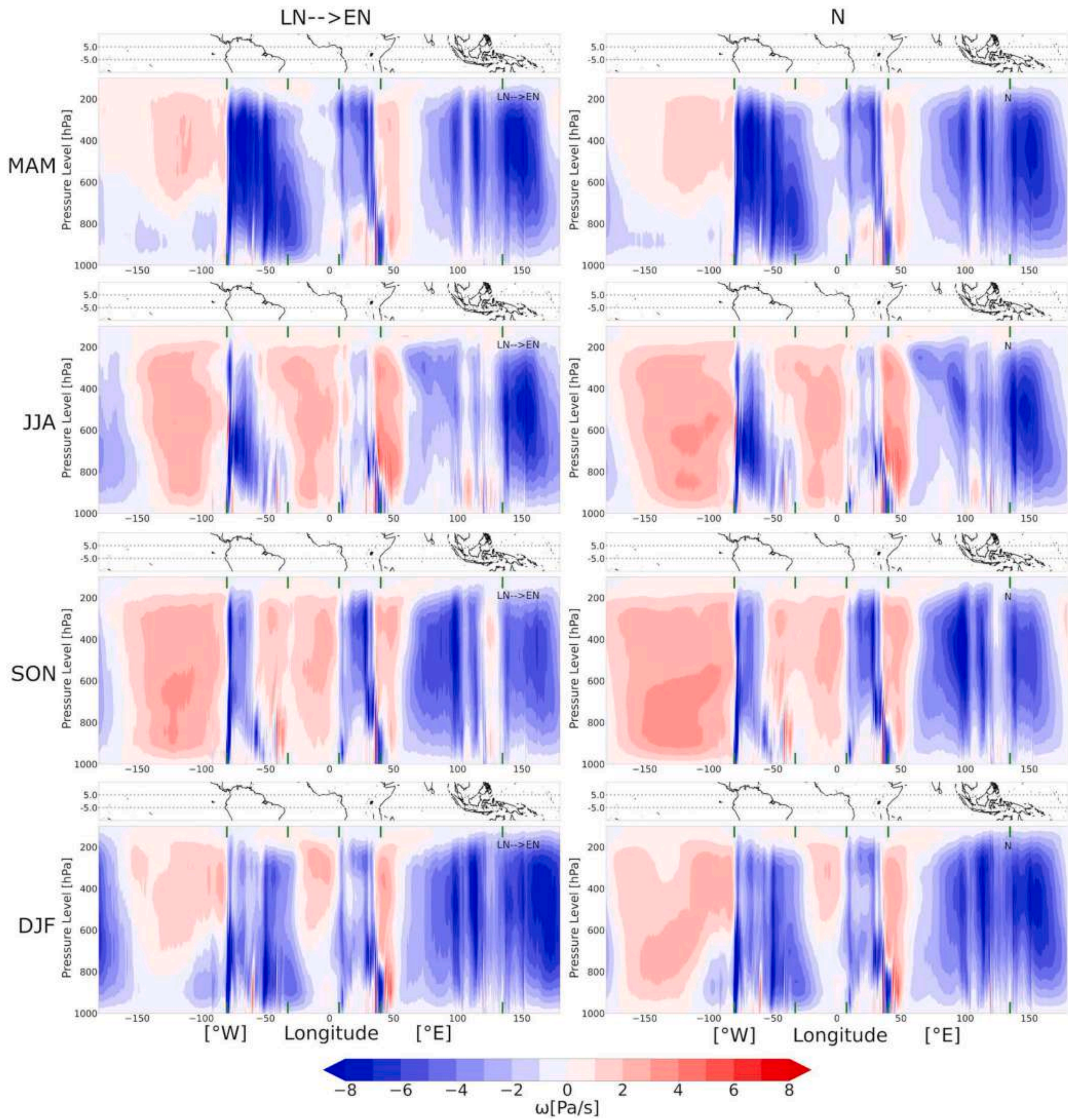

Fig. 12. Seasonal climatology of the vertical velocity of winds, ω, over the 5°N - 5°S region for (left) LN→EN phase transition and (right) N neutral phase.

Fig. 9 the annual cycles of the wind speed cross-section of each low-level jet during transitions and neutral conditions. As a general feature in these cycles, we can observe that during the EN→ LN (LN→ EN) transitions, there is an increase (reduction) of the mean wind speed compared to neutral conditions. In particular, the Chocojet and CLLJ experience higher deviations from neutral conditions, especially during the seasons of their higher activity. Changes in SSTs (Fig. 6) and SST gradients between the FEP facing NSA and the Caribbean may induce changes in the low-level jets in the region. One clear example is the off-season changes of the Chocojet and CLLJ; the former increases its wind speed for both transitions during JJA, while the latter increases its wind speed during SON at the LN→EN transition (Figs. 7 and 9).

5. Conclusions and future work

We studied the influence of ENSO over northern South America using an approach based on the transitions from El Niño (EN) to La Niña (LN) or vice versa. In particular, we investigated the case of the abrupt ENSO transitions from one phase of ENSO to the opposite in one year, from boreal winter to boreal winter. Our approach aims to shed light on the behavior of each transition as an event worth analyzing to examine the variations of the climatology patterns of sea surface temperatures, water vapor transport, and precipitation over northern South America, as well as the wind speeds associated with the Low-Level Jets: Caribbean, Choco, and Orinoco.

Our results evidence that during both ENSO transitions (EN→LN and

LN→EN) for each season there is a set of significant anomalies from the neutral state of ENSO experienced in the region in terms of Sea Surface Temperatures (SST), precipitation, surface wind speeds, and water vapor transport (WVT). In particular, we found that the higher anomalies (positive or negative) during ENSO transitions depend on the location and variable. Notwithstanding, the far-eastern Pacific, the Caribbean sea, the eastern Orinoco, and the northern Amazon river basin exhibit the most notorious changes, which is explained in terms of the fast changes of SST during the transition years from one ENSO phase to another. Furthermore, we point out that the EN→LN (LN→EN) transition shows predominant positive (negative) SST anomalies that remain along the year over the far-eastern Pacific. Nevertheless, the pacific coasts experience increased precipitation in both transitions. Moreover, these climatic anomalies also reveal a precipitation dipole around 5°N over the tropical far-eastern Pacific Ocean, noticeable during both transitions for the JJA and SON seasons.

Fig. 10 provides a schematic representation of the changes observed in the Walker circulation (WC) over the Eastern Pacific (EP) and Northern South America during ENSO transitions. The figure also shows the areas with statistically significant changes in precipitation, SST, and WVT for each season. During the EN→LN (LN→EN) transition, the NSA ascent branch and EP descent branch of the WC exhibit a decreased (increased) pattern. In MAM, the WC over NSA during EN→LN (LN→EN) transition is closer to the EN (LN) canonical phase, while in JJA, the circulation changes abruptly to a pattern more related to LN (EN) canonical phase. This change becomes more consolidated through SON and DJF. Our results suggest that the observed anomalies in precipitation are consistent with the WC patterns found during the ENSO transition phases, where the inhibition (permission) of convection during the EN (LN)-like WC is noted in previous studies (Grimm and Ambrizzi, 2009; Zheleznova and Gushchina, 2017).

Some of the most noticeable features of the anomalies during the phase transitions are the precipitation dipole over the far-eastern pacific which for the EN→LN (LN→EN) transition is found over the ocean (land) during JJA and SON. There is an effect over WVT along the corridors of the Low-level jets. For the EN→LN transition, there is an increased WVT over the Chocojet pathway from MAM to SON, and the OLLJ corridor experiences abrupt changes during the LN→EN transition from SON to DJF that might alter WVT transport from the Orinoco basin to the Amazon basin. Our results show the effect of an abrupt ENSO transition from one phase to another, pointing out their relevance in improving the region's climatic diagnosis and characterization of hydroclimatic processes.

The limitations of our approach based on abrupt ENSO transitions summarizes in four key aspects: (1) this study is based on small samples, which is a limitation for achieving robust statistical results; this limitation also has been documented in other works Bahrami et al. (2020); (2) our results may pose a caveat to be considered in the water planning mainstream, although water availability and the occurrence of droughts and floods are associated with the canonical phases of ENSO, notwithstanding few works study in-depth particularities of the ENSO changes (as transitions focused here), can be associated with the strongest events and impacts in some locations of northern South America; (3) our classification of the ENSO transitions was based only on SST anomalies over the Nino3.4 zone; (4) currently, a transition approach is out of the scope for cases associated with the Central and eastern Pacific types of ENSO, because those considerations would lead to smaller samples than those used in this work. In this sense, although this study presented unprecedented results for northern South America ENSO transitions require further research to be confirmed or rebutted in the future.

Further questions about the ENSO transitions and their regional and local characteristics deserve future work: (1) How are the ENSO transitions in the context of Center Pacific and Eastern Pacific ENSO events?; (2) How Atmospheric-Oceanic Global Climate models simulate the ENSO transitions?; (3) How are ENSO transitions in the context of climate change?; (4) How are other climatic processes (Atlantic Multidecadal Oscillation, Pacific Decadal Oscillation, and others) altered during ENSO transitions?; (5) How is the influence of other types of ENSO transitions?

CRediT authorship contribution statement

Alejandro Builes-Jaramillo: Conceptualization, Methodology, Data-curation, Writing-original-draft. **Juliana Valencia:** Conceptualization, Software, Data-curation, Writing-original-draft. **Hernán D. Salas:** Conceptualization, Data-curation, Methodology, Writing-original-draft.

Declaration of Competing Interest

The authors declare that they have no known competing financial interests or personal relationships that could have appeared to influence the work reported in this paper.

Data availability

Data will be made available on request.

Acknowledgments

The work of A. Builes-Jaramillo and H.D. Salas were supported by Institución Universitaria Colegio Mayor de Antioquia. The work by J. Valencia was supported by the project FAI54 "Características del chorro de bajo nivel del Chocó (ChocoJet) durante el inicio de episodios El Niño" funded by Institución Universitaria Colegio Mayor de Antioquia. The authors would like to thank the European Centre for Medium-Range Weather Forecast ECMWF, which provides freely available ERA5 atmospheric reanalysis datasets.

Appendix A. Vertical velocity climatology

References

Ashok, K., Yamagata, T., 2009. The el niño with a difference. Nature 461, 481–484. https://doi.org/10.1038/461481a.

Bahrami, F., Ranjbar Saadatabadi, A., Meshkatee, A.H., Kamali, G., 2020. The Impact of ENSO Phase Transition on the Atmospheric Circulation, Precipitation and Temperature in the Middle East Autumn. Asia-Pac. J. Atmos. Sci. 56, 439–453. https://doi.org/10.1007/s13143-019-00149-2.

Bayr, T., Dommenget, D., Latif, M., 2020. Walker circulation controls ENSO atmospheric feedbacks in uncoupled and coupled climate model simulations. Clim. Dyn. 54, 2831–2846. https://doi.org/10.1007/s00382-020-05152-2.

Bayr, T., Latif, M., Dommenget, D., Wengel, C., Harlaß, J., Park, W., 2018. Mean-state dependence of ENSO atmospheric feedbacks in climate models. Clim. Dyn. 50, 3171–3194. https://doi.org/10.1007/s00382-017-3799-2.

Bjerknes, J., 1969. Atmospheric teleconnections from the Equatorial Pacific. Mon. Weather Rev. 97, 163–172. https://doi.org/10.1175/1520-0493(1969)097<0163:ATFTEP>2.3.CO;2. URL:http://journals.ametsoc.org/doi/10.1175/1520-0493(1969)097%3C0163:ATFTEP%3E2.3.CO;2.

Boschat, G., Simmonds, I., Purich, A., Cowan, T., Pezza, A.B., 2016. On the use of composite analyses to form physical hypotheses: An example from heat wave - SST associations. Sci. Rep. 6, 1–10. https://doi.org/10.1038/srep29599. URL:https://www.exelisvis.com/.

Brahmananda Rao, V., Chapa, S.R., Cavalcanti, I.F., 1998. Moisture budget in the tropics and the Walker circulation. J. Geophys. Res. Atmos. 103, 13713–13728. https://doi.org/10.1029/98jd00943.

Builes-Jaramillo, A., Yepes, J., Salas, H.D., 2022. The Orinoco Low-Level Jet and Its Association with the Hydroclimatology of Northern South America. J. Hydrometeorol. 23, 209–223. https://doi.org/10.1175/JHM-D-21-0073.1. URL: https://journals.ametsoc.org/view/journals/hydr/aop/JHM-D-21-0073.1/JHM-D-21-0073.1.xmlhttps://journals.ametsoc.org/view/journals/hydr/23/2/JHM-D-21-0073.1.xml.

Builes-Jaramillo, A., Yepes, J., Salas, H.D., 2022. The Orinoco low-level jet during El Niño-Southern Oscillation. Int. J. Climatol. 10, 1–15. https://doi.org/10.1002/joc.7681. URL:https://onlinelibrary.wiley.com/doi/10.1002/joc.7681.

Cai, W., McPhaden, M.J., Grimm, A.M., Rodrigues, R.R., Taschetto, A.S., Garreaud, R.D., Dewitte, B., Poveda, G., Ham, Y.G., Santoso, A., Ng, B., Anderson, W., Wang, G., Geng, T., Jo, H.S., Marengo, J.A., Alves, L.M., Osman, M., Li, S., Wu, L., Karamperidou, C., Takahashi, K., Vera, C., 2020. Climate impacts of the el niño–southern oscillation on south america. Nat. Rev. Earth Environ. 1, 215–231. https://doi.org/10.1038/s43017-020-0040-3.

de Carvalho, L.M.V., Cavalcanti, I.F.A., 2016. The South American Monsoon System (SAMS), pp. 121–148. URL:http://link.springer.com/10.1007/978-3-319-21650-8_6, doi:10.1007/978-3-319-21650-8_6.

Cerón, W.L., Andreoli, R.V., Kayano, M.T., de Souza, R.A.F., Jones, C., Carvalho, L.M., 2020. The influence of the atlantic multidecadal oscillation on the choco low-level jet and precipitation in colombia. Atmosphere 11. https://doi.org/10.3390/atmos11020174.

Diaz, H.F., Hoerling, M.P., Eischeid, J.K., 2001. Enso variability, teleconnections and climate change. Int. J. Climatol. 21, 1845–1862. https://doi.org/10.1002/joc.631.

Enfield, D.B., Mayer, D.a., 1997. Tropical Atlantic sea surface temperature variability and its relation to El Niño-Southern Oscillation. J. Geophys. Res. 102, 929–945.

Fang, S.W., 2020. Understanding ENSO Transition Complexity and its Underlying Dynamics. Ph.D. thesis. University of California, Irvine. URL:http://dissertations.umi.com/uci:16346.

Giannini, A., Chiang, J.C.H., Cane, M.a., Kushnir, Y., Seager, R., 2001. The ENSO teleconnection to the Tropical Atlantic Ocean: Contributions of the remote and local SSTs to rainfall variability in the Tropical Americas. J. Clim. 14, 4530–4544. https://doi.org/10.1175/1520-0442(2001)014<4530:tetttt>2.0.co;2.

Gill, A.E., 1980. Some simple solutions for heat-induced tropical circulation. Q. J. R. Meteorol. Soc. 106, 447–462. https://doi.org/10.1002/qj.49710644905. URL: https://onlinelibrary.wiley.com/doi/10.1002/qj.49710644905.

Glantz, M.H., Ramirez, I.J., 2020. Reviewing the oceanic niño index (oni) to enhance societal readiness for el niño's impacts. Int. J. Disaster Risk Sci. 11, 394–403. https://doi.org/10.1007/s13753-020-00275-w.

Grimm, A.M., Ambrizzi, T., 2009. Teleconnections into South America from the Tropics and Extratropics on Interannual and Intraseasonal Timescales. In: Past Climate Variability in South America and Surrounding Regions From the Last Glacial Maximum to the Holocene. Springer, pp. 159–191. https://doi.org/10.1007/978-90-481-2672-9_7. URL:http://link.springer.com/10.1007/978-90-481-2672-9_7.

Grimm, A.M., Tedeschi, R.G., 2009. Enso and extreme rainfall events in south america. J. Clim. 22, 1589–1609. https://doi.org/10.1175/2008JCLI2429.1.

Guilyardi, E., Wittenberg, A., Fedorov, A., Collins, M., Wang, C., Capotondi, A., van Oldenborgh, G.J., Stockdale, T., 2009. Understanding El Niño in ocean-atmosphere general circulation models: Progress and challenges. Bull. Am. Meteorol. Soc. 90, 325–340. https://doi.org/10.1175/2008BAMS2387.1.

Hersbach, H., Bell, B., Berrisford, P., Hirahara, S., Horányi, A., Muñoz-Sabater, J., Nicolas, J., Peubey, C., Radu, R., Schepers, D., Simmons, A., Soci, C., Abdalla, S., Abellan, X., Balsamo, G., Bechtold, P., Biavati, G., Bidlot, J., Bonavita, M., De Chiara, G., Dahlgren, P., Dee, D., Diamantakis, M., Dragani, R., Flemming, J., Forbes, R., Fuentes, M., Geer, A., Haimberger, L., Healy, S., Hogan, R.J., Hólm, E., Janisková, M., Keeley, S., Laloyaux, P., Lopez, P., Lupu, C., Radnoti, G., de Rosnay, P., Rozum, I., Vamborg, F., Villaume, S., Thépaut, J.N., 2020. The ERA5 global reanalysis. Q. J. R. Meteorol. Soc. 146, 1999–2049. https://doi.org/10.1002/qj.3803.

Mokhov, I.I., Timazhev, A.V., 2022. Seasonal Temperature Extremes in the North Eurasian Regions Depending on ENSO Phase Transitions. Atmosphere 13. https://doi.org/10.3390/atmos13020249.

Nesbitt, S.W., Salio, P.V., Ávila, E., Bitzer, P., Carey, L., Chandrasekar, V., Deierling, W., Dominguez, F., Dillon, M.E., Garcia, C.M., Gochis, D., Goodman, S., Hence, D.A., Kosiba, K.A., Kumjian, M.R., Lang, T., Luna, L.M., Marquis, J., Marshall, R., McMurdie, L.A., de Lima Nascimento, E., Rasmussen, K.L., Roberts, R., Rowe, A.K., Ruiz, J.J., São Sabbas, E.F., Saulo, A.C., Schumacher, R.S., Skabar, Y.G., Toledo Machado, L.A., Trapp, R.J., Varble, A.C., Wilson, J., Wurman, J., Zipser, E.J., Arias, I., Bechis, H., Grover, M.A., 2021. A Storm Safari in Subtropical South America: Proyecto RELAMPAGO. Bull. Am. Meteorol. Soc. 102, E1621–E1644. https://doi.org/10.1175/BAMS-D-20-0029.1. URL:https://journals.ametsoc.org/view/journals/bams/102/8/BAMS-D-20-0029.1.xml.

NOAA, 2022. Cold and warm episodes by season.

Oliver, J.E., 2005. Walker circulation. Encycl. Earth Sci. Ser. 797–798. https://doi.org/10.1007/1-4020-3266-8_223.

Ordóñez-Zúñiga, S.A., Correa-Ramírez, M., Ricaurte-Villota, C., Bastidas-Salamanca, M., 2021. The Panama Low-Level Jet: extension, annual cycle and modes of variation. Lat. Am. J. Aquat. Res. 49, 750–762. https://doi.org/10.3856/vol49-issue5-fulltext-2591.

Philander, S.G., 1990. The Southern Oscillation: Variability of the Tropical Atmosphere. In: El Niño, La Niña, and the Southern Oscillation, pp. 9–57. URL:https://linkinghub.elsevier.com/retrieve/pii/S0074614208601722, doi:10.1016/S0074-6142(08)60172-2.

Philander, S.G.H., 1983. El niño southern oscillation phenomena. Nature 302, 295–301. https://doi.org/10.1038/302295a0.

Poveda, G., Álvarez, D.M., Rueda, Óscar A., 2011. Hydro-climatic variability over the andes of colombia associated with enso: a review of climatic processes and their impact on one of the earth's most important biodiversity hotspots. Clim. Dyn. 36, 2233–2249. https://doi.org/10.1007/s00382-010-0931-y.

Rayner, N.A., Parker, D.E., Horton, E.B., Folland, C.K., Alexander, L.V., Rowell, D.P., Kent, E.C., Kaplan, A., 2003. Global analyses of sea surface temperature, sea ice, and night marine air temperature since the late nineteenth century. J. Geophys. Res. 108, 4407. https://doi.org/10.1029/2002JD002670. URL:http://doi.wiley.com/10.1029/2002JD002670.

Romero-Centeno, R., Zavala-Hidalgo, J., Raga, G.B., 2007. Midsummer gap winds and low-level circulation over the eastern tropical Pacific. J. Clim. 20, 3768–3784. https://doi.org/10.1175/JCLI4220.1.

Sarachik, E.S., Cane, M.A., 2010. The El Niño–Southern Oscillation Phenomenon. Cambridge University Press. https://doi.org/10.1017/CBO9780511817496.

Saravanan, R., Chang, P., 2000. Interaction between tropical Atlantic variability and El Nino-Southern Oscillation. J. Clim. 13, 2177–2194. https://doi.org/10.1175/1520-0442(2000)013<2177:IBTAVA>2.0.CO;2.

Sasaki, C.R.S., Rowe, A.K., McMurdie, L.A., Rasmussen, K.L., 2022. New Insights into the South American Low-Level Jet from RELAMPAGO Observations. Mon. Weather Rev. 150, 1247–1271. https://doi.org/10.1175/MWR-D-21-0161.1. URL:https://journals.ametsoc.org/view/journals/mwre/150/6/MWR-D-21-0161.1.xml.

Sasaki, W., Doi, T., Richards, K.J., Masumoto, Y., 2015. The influence of ENSO on the equatorial Atlantic precipitation through the Walker circulation in a CGCM. Clim. Dyn. 44, 191–202. https://doi.org/10.1007/s00382-014-2133-5.

Serna, L.M., Arias, P.A., Vieira, S.C., 2018. Las corrientes superficiales de chorro del Chocó y el Caribe durante los eventos de El Niño y El Niño Modoki. Rev. Acad. Colomb. Cienc. Exactas, Físicas y Naturales 42, 410. https://doi.org/10.18257/raccefyn.705.

Shi, W., Huang, S., Liu, D., Huang, Q., Han, Z., Leng, G., Wang, H., Liang, H., Li, P., Wei, X., 2021. Drought-flood abrupt alternation dynamics and their potential driving forces in a changing environment. J. Hydrol. 597, 126179 https://doi.org/10.1016/j.jhydrol.2021.126179. URL:https://linkinghub.elsevier.com/retrieve/pii/S0022169421002262.

Sierra, J.P., Arias, P.A., Durán-Quesada, A.M., Tapias, K.A., Vieira, S.C., Martínez, J.A., 2021. The Choco low-level jet: past, present and future. Clim. Dyn. 56, 2667–2692. https://doi.org/10.1007/s00382-020-05611-w.

Tedeschi, R.G., Sampaio, G., 2022. Influences of different intensities of El Niño-Southern Oscillation on South American precipitation. Int. J. Climatol. 1–21 https://doi.org/10.1002/joc.7688.

Wang, C., 2007. Variability of the Caribbean Low-Level Jet and its relations to climate. Clim. Dyn. 29, 411–422. https://doi.org/10.1007/s00382-007-0243-z.

Wang, C., Picaut, J., 2013. Understanding Enso Physics-A Review, pp. 21–48. https://doi.org/10.1029/147GM02. URL:https://onlinelibrary.wiley.com/doi/10.1029/147GM02.

Wang, J., Rong, G., Li, K., Zhang, J., 2021. Analysis of Characteristics of Dry-Wet Events Abrupt Alternation in Northern Shaanxi, China. Water 13, 2384. https://doi.org/10.3390/w13172384. URL:https://www.mdpi.com/2073-4441/13/17/2384.

Warner, S.J., Moum, J.N., 2019. Feedback of Mixing to ENSO Phase Change. Geophys. Res. Lett. 46, 13920–13927. https://doi.org/10.1029/2019GL085415.

Wu, B., Zhou, T., Li, T., 2009. Contrast of rainfall-SST relationships in the western North Pacific between the ENSO-developing and ENSO-decaying summers. J. Clim. 22, 4398–4405. https://doi.org/10.1175/2009JCLI2648.1.

Xie, Z., Duan, A., Tian, Q., 2017. Weighted composite analysis and its application: an example using ENSO and geopotential height. Atmos. Sci. Lett. https://doi.org/10.1002/asl.786.

Yepes, J., Poveda, G., Mejía, J.F., Moreno, L., Rueda, C., 2019. Choco-jex: A research experiment focused on the Chocó low-level jet over the far eastern Pacific and western Colombia. Bull. Am. Meteorol. Soc. 100, 779–796. https://doi.org/10.1175/BAMS-D-18-0045.1.

Zheleznova, I.V., Gushchina, D.Y., 2017. Hadley and Walker circulation anomalies associated with the two types of El Niño. Russ. Meteorol. Hydrol. 42, 625–634. https://doi.org/10.3103/S1068373917100016.

Alejandro Builes-Jaramillo is a Doctor in Engineering - Water Resources, Master in Engineering, and Civil Engineer. With experience in research on long-term water balances in large-scale hydrological basins, analysis of hydroclimatological systems with tools from nonlinear systems theory, and analysis of natural resources and socio-environmental systems for urban environmental management. Since 2011 he has been a full-time professor of the Environmental Engineering program at the Institución Universitaria Colegio Mayor de Antioquia in the city of Medellín.

Juliana Valencia is an Environmental Engineer with experience in processing and analysis of hydroclimatological and meteorological data. Since 2019, she has been a young researcher at the Institución Universitaria Colegio Mayor de Antioquia in Medellín, Colombia.

Hernán D. Salas is a Doctor in Water Resources Engineering, Master in Engineering, and Civil Engineer. His research is focused on hydrology, hydro-climatology, and nonlinear techniques applied to analyze hydro-climatic processes and water resources systems for social, environmental, and economical purposes. Since 2019 is a professor for the Environmental Engineering program at the Institución Universitaria Colegio Mayor de Antioquia in Medellín, Colombia.

MINISTERIO DE CIENCIA, TECNOLOGÍA E INNOVACIÓN

publindex INDEXACIÓN – HOMOLOGACIÓN

LISTADO REVISTAS HOMOLOGADAS

No.	NOMBRE	ISSN	CATEGORIA	VIGENCIA	LISTA_SIR
1595	TRENDS IN GENETICS	0168-9525; 1362-4555	A1	Enero 2023 - Julio 2023	Index Medicus; Scimago Journal Rank - SJR; Journal Citation Reports - JCR
1596	APPLIED CLAY SCIENCE	0169-1317; 1872-9053	A1	Enero 2023 - Julio 2023	Scimago Journal Rank - SJR; Journal Citation Reports - JCR
1597	ORE GEOLOGY REVIEWS	0169-1368; 1872-7360	A1	Enero 2023 - Julio 2023	Scimago Journal Rank - SJR; Journal Citation Reports - JCR
1598	LANDSCAPE AND URBAN PLANNING	0169-2046; 1872-6062	A1	Enero 2023 - Julio 2023	Scimago Journal Rank - SJR; Journal Citation Reports - JCR
1599	INTERNATIONAL JOURNAL OF FORECASTING	0169-2070; 1872-8200	A1	Enero 2023 - Julio 2023	Scimago Journal Rank - SJR; Journal Citation Reports - JCR
1600	COMPUTER METHODS AND PROGRAMS IN BIOMEDICINE	0169-2607; 1872-7565	A1	Enero 2023 - Julio 2023	Index Medicus; Scimago Journal Rank - SJR; Journal Citation Reports - JCR
1601	SURVEYS IN GEOPHYSICS	0169-3298; 1573-0956	A1	Enero 2023 - Julio 2023	Scimago Journal Rank - SJR; Journal Citation Reports - JCR
1602	BIOLOGY PHILOSOPHY	0169-3867; 1572-8404	A1	Enero 2023 - Julio 2023	Arts and Humanities Citation Index (AHCI); Scimago Journal Rank - SJR; Journal Citation Reports - JCR
1603	TRANSPORT IN POROUS MEDIA	0169-3913; 1573-1634	A1	Enero 2023 - Julio 2023	Scimago Journal Rank - SJR; Journal Citation Reports - JCR
1604	ADVANCED DRUG DELIVERY REVIEWS	0169-409X; 1872-8294	A1	Enero 2023 - Julio 2023	Scimago Journal Rank - SJR; Journal Citation Reports - JCR
1605	NEW FORESTS	0169-4286; 1573-5095	A1	Enero 2023 - Julio 2023	Scimago Journal Rank - SJR; Journal Citation Reports - JCR
1606	APPLIED SURFACE SCIENCE	0169-4332; 1873-5584	A1	Enero 2023 - Julio 2023	Scimago Journal Rank - SJR; Journal Citation Reports - JCR
1607	LUNG CANCER	0169-5002; 1872-8332	A1	Enero 2023 - Julio 2023	Index Medicus; Scimago Journal Rank - SJR; Journal Citation Reports - JCR
1608	AGRICULTURAL ECONOMICS	0169-5150; 1574-0862	A1	Enero 2023 - Julio 2023	Scimago Journal Rank - SJR; Journal Citation Reports - JCR
1609	TRENDS IN ECOLOGY EVOLUTION	0169-5347; 1872-8383	A1	Enero 2023 - Julio 2023	Scimago Journal Rank - SJR; Journal Citation Reports - JCR
1610	GEOMORPHOLOGY	0169-555X; 1872-695X	A1	Enero 2023 - Julio 2023	Scimago Journal Rank - SJR; Journal Citation Reports - JCR
1611	CHEMOMETRICS AND INTELLIGENT LABORATORY SYSTEMS	0169-7439; 1873-3239	A1	Enero 2023 - Julio 2023	Scimago Journal Rank - SJR; Journal Citation Reports - JCR
1612	JOURNAL OF CONTAMINANT HYDROLOGY	0169-7722; 1873-6009	A1	Enero 2023 - Julio 2023	Scimago Journal Rank - SJR; Journal Citation Reports - JCR
1613	ATMOSPHERIC RESEARCH	0169-8095; 1873-2895	A1	Enero 2023 - Julio 2023	Scimago Journal Rank - SJR; Journal Citation Reports - JCR
1614	MATHEMATICAL METHODS IN THE APPLIED SCIENCES	0170-4214; 1099-1476	A1	Enero 2023 - Julio 2023	Scimago Journal Rank - SJR; Journal Citation Reports - JCR